Rock and Soil Mechanics

Volume 42 | Issue 10 Article 1

1-12-2022

Pore structure and strength deterioration mechanism of phase change energy storage backfill

Ai-bing JIN
School of Civil and Resource Engineering, University of Science and Technology Beijing, Beijing 100083, China

You JU
School of Civil and Resource Engineering, University of Science and Technology Beijing, Beijing 100083, China

Hao SUN
School of Civil and Resource Engineering, University of Science and Technology Beijing, Beijing 100083, China, sunhao2019@ustb.edu.cn

Yi-qing ZHAO
School of Civil and Resource Engineering, University of Science and Technology Beijing, Beijing 100083, China

See next page for additional authors

Custom Citation

JIN Ai-bing, JU You, SUN Hao, ZHAO Yi-qing, LI Hai, ZHANG Zhou, LU Tong, . Pore structure and strength deterioration mechanism of phase change energy storage backfill[J]. Rock and Soil Mechanics, 2021, 42(10): 2623-2633.

Pore structure and strength deterioration mechanism of phase change energy storage backfill

Authors

Ai-bing JIN, You JU, Hao SUN, Yi-qing ZHAO, Hai LI, Zhou ZHANG, and Tong LU

Rock and Soil Mechanics 2021 42(10): 2623−2633 ISSN 1000−7598
https: //doi.org/10.16285/j.rsm.2021.5541 rocksoilmech.researchcommons.org/journal

Pore structure and strength deterioration mechanism of phase change energy storage backfill

JIN Ai-bing[1, 2], JU You[1, 2], SUN Hao[1, 2], ZHAO Yi-qing[1, 2], LI Hai[1, 2], ZHANG Zhou[1, 2], LU Tong[1, 2]

1. Key Laboratory of Ministry of Education for Efficient Mining and Safety of Metal Mines, University of Science and Technology Beijing, Beijing 100083, China
2. School of Civil and Resource Engineering, University of Science and Technology Beijing, Beijing 100083, China

Abstract: In order to explore the pore structure characteristics of phase change energy storage backfill and their influence on the strength deterioration of backfill, a composite phase change material was prepared with butyl stearate as the phase change material and expanded perlite as the adsorption medium. Cement and tailings were mixed to prepare backfills with different additive amounts of the composite phase change material. The strength and structure characteristics of the phase change energy storage backfill with different addition amounts were obtained by using the methods of CT (computer tomography) scanning, MRI (magnetic resonance imaging) analysis, and uniaxial compression test, and the influence mechanism was analyzed. The results show that: i) The porosity of phase change energy storage backfill increases gradually with the increase of the addition amount. The macropore porosity increases approximately linearly, the proportion of macropores increases gradually, and the pores approximate to sphere. ii) With the increase of the amount of phase change material, the connectivity of the backfill increases, the pore throat length increases, and the number of macropores increases. The pore throat coordination number is concentrated below 5, and the fractal dimension decreases first and then increases significantly, resulting in complex pore distribution. iii) With 5% additive amount, the uniaxial compressive strength of backfill decreases by 30.2% due to the increase of macropores and pore connectivity. With 10% additive amount, the pore size distribution becomes uniform and the uniaxial compressive strength decreases by 48.9%.

Keywords: phase change materials; backfill; pore characteristics; CT scan; magnetic resonance imaging; uniaxial compressive strength

1 Introduction

The phase change energy storage backfills (hereinafter referred to as “phase change backfill”) made of filling and sealing material evenly mixed with phase change material can improve the high ground temperature environment[1−2], and has good heat storage performance, but its strength will severely deteriorate with the increase of the composite material additive amount[3−6]. The backfills used in mines are required to meet certain strength conditions. However, during the phase change, the composite material is not engaged in chemical reactions or property changes with the filling material, thus the strength degradation might be mainly caused by the increased porosity after being mixed with porous medium, and inherently, the complex pore distribution results in severe strength degradation during loading process[7−8]. Therefore, to investigate the strength degradation mechanism of phase change backfill, it is necessary to analyze its characteristics when mixed with different additive amounts, including the pore quantity, volume and distribution.

The main methods used to study pore characteristics of materials such as rock masses or specimens include scanning electron microscope (SEM) observation, magnetic resonance imaging (MRI), and computed tomography (CT). To obtain the pore characteristics, Jiang et al.[9] performed SEM scanning on different groups of calcareous sand and analyzed the porosity and connected pores of calcareous sand with Matlab binarization. Zhao et al.[10] used SEM to observe the microstructure of sandstone at different temperatures, and the pore expanding and connecting process with temperature is obtained. Liu et al.[11] conducted MRI tests on sandstone before and after freezing and thawing, and the change of the sandstone pore structure with the freezing and thawing treatment is obtained, and the strength enhancement mechanism of frozen rocks is proposed. Jin et al.[12] used MRI to obtain the internal pore size distribution and pore changes of high-temperature sandstone under different cooling conditions, and analyzed the relationship between pore characteristics and temperature conditions, and the process of pore connecting and expanding into cracks. Since CT scan can accurately obtain the pore characteristics, it has been widely used

Received: 13 April 2021 Revised: 22 June 2021
This work was supported by the National Natural Science Foundation of China (52004017), the China Postdoctoral Science Foundation Project (2020M670138) and the Fundamental Research Funds for the Central Universities Project (FRF-TP-19-026A1).
First author: JIN Ai-bing Jin, male, born in 1974, PhD, Professor, mainly engaged in the teaching and research works in rock mechanics and engineering. E-mail: jinaibing@ustb.edu.cn
Corresponding author: SUN Hao, male, born in 1992, PhD, Lecturer, mainly engaged in the teaching and research works in rock mechanics and mining technology and theory. E-mail: sunhao2019@ustb.edu.cn

by scholars to analyze the microstructure of rock and concrete specimens[13−16].Fu et al.[17] used CT scanning and three-dimensional (3D) reconstruction to obtain the 3D model of coal mineral structure, and performed a series of compression simulations with the numerical models containing different diameter ranges of minerals, and obtained the influence of mineral content and distribution on strength and failure. Liu et al.[18] obtained the 3D images of sandy loam soil treated with different freeze−thaw cycles through CT scanning, and obtained the relationship between pore characteristics and freeze- thaw swelling.

By using CT scanning, the binarized images of pores can be obtained, and the pore structures can be analyzed and the pore network model can be built with the 3D reconstruction. With these operations, the basic pore characteristics (quantity, size and shape), pore connectivity characteristics (number of pore throat, pore throat length and pore throat coordination number) and the pore distribution characteristics (fractal dimension) can be thoroughly analyzed[19−20]. Chen et al.[21] processed the concrete with different recycled aggregate addition rates based on CT technology and extracted the 3D structure of the pores in the concrete. Research results show that the pore structure characteristics including porosity, pore size, and pore shape have a great correlation with concrete strength. Chen et al.[22] performed CT scanning on 6 groups of basalt fiber concrete with different fiber contents and established a pore structure model and a fiber distribution model, and the results indicate pore structure and its connectivity are conducive to the improvement of concrete performance. Wang et al.[23] and Peng et al.[24] used CT scanning technology to process coal specimens and various rock specimens, and reconstructed the structural characteristics of their pores and cracks. Fractal dimension was used to determine the complexity of pore distribution and the structural characteristics. Gerke et al.[25] improved the pore network structure construction method based on the maximum inscribed sphere algorithm and proposed a new method which was then applied to the watershed calculation. Wildenschild et al.[26], Muljadi et al.[27] and Khan et al.[28] applied CT scanning technology to the study of pore acquisition and multiphase flow characteristics in the porous medium, investigated the applications of pore network structure acquisition, and proposed the pore network structure extraction method based on watershed algorithms.

Jin et al.[29] investigated the influencing factors of the strength of the phase change backfill and found that the backfill strength will gradually deteriorate as the additive amount of the phase change material increases from 0% to 15%, and the backfill strength reduces by more than 50% when the additive amount is 15%. According to the SEM results, the main reason for the strength deterioration is that the pore structure changes as the addition amount increases. Based on the previous research results, the 15% additive amount is discarded when preparing the phase change backfill as it would cause severe strength deterioration. After comprehensive analysis, expanded perlite (EP) is used to adsorb n-butyl stearate (BS) to prepare the composite phase change material. The cement sand ratio of filling material is 1:4, the slurry concentration is 70%, and three groups of composite phase change materials with the mass fractions of 0%, 5% and 10% are prepared. These composite phase change materials are used to study the characteristics of pore structure and their influence on the strength degradation mechanism. Because of the respective limitations of MRI and CT as the former cannot obtain complete spatial distribution of pores, and the latter cannot obtain the distribution of fine pores due to resolution limitation, a two-step acquisition method is adopted, which firstly uses CT scanning to obtain the basic pore characteristics, connectivity and distribution characteristics of the backfill pores, and then combines with the MRI results to optimize the basic characteristics of pores (porosity, pore size distribution) obtained from CT scanning. Then, uniaxial compression tests are performed on phase change backfill with different additions to obtain their uniaxial compressive strength, and to investigate the correlation between pore characteristics and strength deterioration. This study is important to the understanding of the mechanism of phase change materials affecting backfill strength. It facilitates future research on strength degradation mitigation and thermal performance improvement of the phase change backfill.

2 Test materials and solutions

2.1 Experiment materials

Materials include the Butyl stearate of 99% purity, expanded perlite with the particle size of 3–5 mm, white latex, standard cement, iron-ore tailing sand, and tap water.

2.2 Preparation of phase change backfill

The composite phase change material is prepared according to the following steps: (1) Remove moisture by placing the expanded perlite in an oven and bake for 24 hours at high temperature; (2) put an appropriate amount of pretreated expanded perlite in a 500 mL suction filter flask, set a constant-temperature water bath at 40 °C, and add excess liquid butyl stearate, then perform vacuum filtration repeatedly for 30 minutes before removing the expanded perlite; and (3) spread the surface of expanded perlite evenly with white latex, let it stand for 6 hours, and the BS/EP composite phase

change material (for convenience of explanation, hereinafter referred to as BS/EP-CPCM) is prepared after the white latex is dry and solidified.

The cement sand ratio of filling material is 1:4, the slurry concentration is 70%, and three groups of composite phase change materials with the mass fractions of 0%, 5% and 10% are prepared. The specific proportions are shown in Table 1.

Table 1 Backfill proportion and mass

BS/EP-CPCM additive amount /%	Cement /g	Tailing sand /g	Water /g	BS/EP-CPCM /g
0	190	760	407.1	0
5	190	722	407.1	38
10	190	684	407.1	76

The masses of cement, tailing sand, water and BS/EP-CPCM are respectively weighed according to the proportions listed in Table 1. After intimate mixing, they are poured into a standard cylindrical mold (ϕ50 mm× 100 mm) to prepare cylindrical specimens. The inner surface of the mold is evenly coated with lubricating oil for demolding. After standing for 24 hours, the demolded specimens are individually labeled and placed in a curing chamber to be cured at a constant temperature of 19 ℃ and a humidity of 97% for 28 days. The finished phase change backfill specimens are shown in Fig. 1.

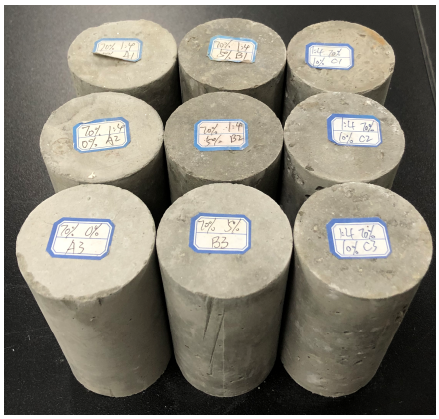

Fig. 1 Cylindrical specimen of phase change energy storage backfill

2.3 CT scanning and pore network construction

The instrument used for CT scanning is the NanoVoxel-3800E micro-CT scanning system (see Fig. 2), and its maximum scanning range is 300 mm×300 mm× 100 mm. Three specimens of the phase change backfill with different BS/EP-CPCM percentages are selected and individually placed and fixed on the stage. The size of the test specimen is ϕ50 mm×100 mm, the scanning voltage is 170 kV, the current is 40 μA, and SQ spiral scanning mode is adopted. The scanning conditions of the three specimens remain exactly the same. The scanning frame number is 1 080 and the resolution is 31.4 μm. The scanning time of a single specimen is 120 min.

After the scanning is completed, vertical and horizontal slices of the phase change backfill body are obtained. The pixel size of the horizontal slice is 1 650 pixels × 1 650 pixels. Data reconstruction is conducted by importing the obtained CT scanning data into the Voxel Studio Recon software. First, the transverse slice range is selected according to the required size. Then, parameter adjustment, geometric correction and hardening correction are performed. Finally, the three-dimensional reconstructed images are outputted.

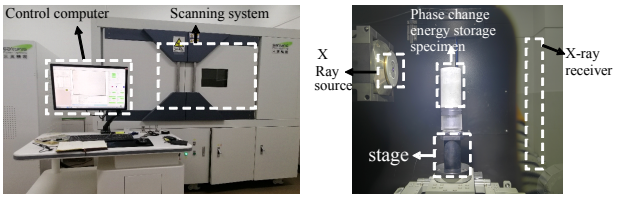

(a) CT scanning device (b) Scanning system

Fig. 2 Schematic diagram of CT scanning system

2.4 MRI

Three specimens of the phase change backfill with different BS/EP-CPCM percentages are taken to carry out water saturation treatment via the vacuum pressure water retention equipment. When saturated with water, the air in the rock core chamber is pumped out until the vacuum value is −0.1 MPa. After the pumping is completed, the specimen in the core chamber is immersed in distilled water for 24 hours to make a saturated backfill.

After the water saturation is completed, the MesoMR23-060H-I nuclear magnetic resonance instrument (see Fig. 3) is used to perform nuclear magnetic resonance test on the specimens. The porosity and pore size distribution of the phase change backfill bodies with different BS/EP-CPCM additive amounts are obtained.

Fig. 3 MesoMR23-060H-I magnetic resonance imaging analyzer

2.5 Uniaxial compression test

The specimens of the phase change backfill are cured for 28 days and polished afterwards to prepare for the uniaxial compression test. The test is conducted using the YAW-600 compression testing machine (see Fig. 4). The displacement control mode is adopted, the loading rate is 0.001 mm/s, and the average value of three specimens is taken as the uniaxial compressive strength.

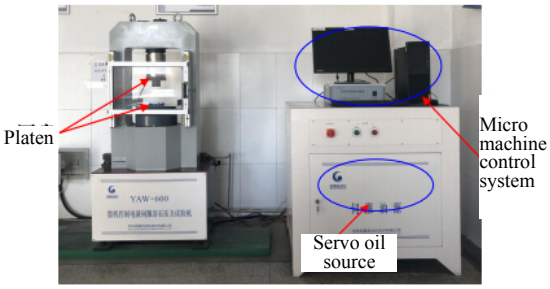

Fig. 4 YAW-600 rock pressure testing machine

3 Test results and analysis

According to the results of different experiments, the following section analyzes the CT scanning pore characteristics, MRI pore characteristics, uniaxial compressive strength, and porosity-influencing strength deterioration mechanism of phase change backfill with different additive amounts.

3.1 Pore characteristics obtained by CT scanning

3.1.1 Image processing and pore structure acquisition

In order to obtain the internal pore characteristics of the phase change backfill with different BS/EP-CPCM additions, it is necessary to process the data obtained by CT scanning, extract the pore characteristics, and construct pore network model to obtain the pore connectivity. The three-dimensional images of the pores and pore throat characteristics obtained with different BS/EP-CPCM additions are shown in Fig. 5.

3.1.2 Basic pore characteristics

The basic pore characteristics obtained by CT scanning include porosity, pore size, and pore sphericity which characterizes the three-dimensional shape of the pores. The analyses of the basic pore characteristics of the phase change backfill with different BS/EP-CPCM additive amounts are as follows. At present, pores are generally divided into micropores (<1 μm), mesopores (1–10 μm) and macropores (>10 μm) according to the pore size[30]. Since the resolution of CT scanning is 31.4 μm, processing CT images can only obtain the characteristics of macropores. The following CT scanning results are mainly used to analyze the laws of macropores. The complete pore size distribution and influence will be investigated in conjunction with MRI results.

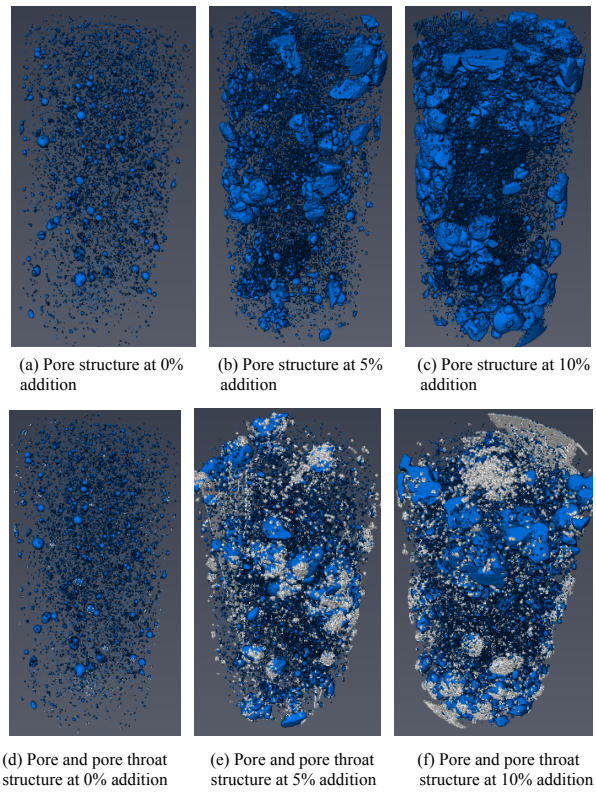

Fig. 5 Pore and pore throat structures of backfill with different additive amounts

(1) Macropore ratio

The porosity and pore quantity of the backfill can be obtained by analyzing the slices generated by the threshold segmentation. The comparison of the macropore ratio and the number of pores of the phase change backfill with different additive amounts is shown in Fig. 6.

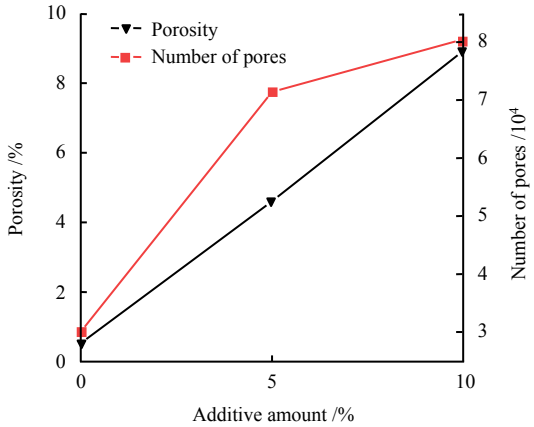

Fig. 6 Pore and pore throat structure of backfill with different additive amounts

Figure 6 shows that when the additive amount of BS/EP-CPCM is 0%, the phase change backfill contains 30 145 macropores and the porosity is 0.53%; when the additive amount is 5%, the backfill contains 71 481 macropores and the porosity is 4.61%; and when the additive amount is 10%, the backfill contains 80 570

macropores and the porosity is 8.92%. The macropore ratio increases linearly with the increase of the addition of BS/EP-CPCM. However, when the additive amount is 5%, the number of macropores increases comparatively greatly, and the number of internal pores is relatively large, while the pore volume is relatively small.

(2) Macropore size

Figure 7 shows the distribution of the macropore size of the phase change backfill with different additive amounts.

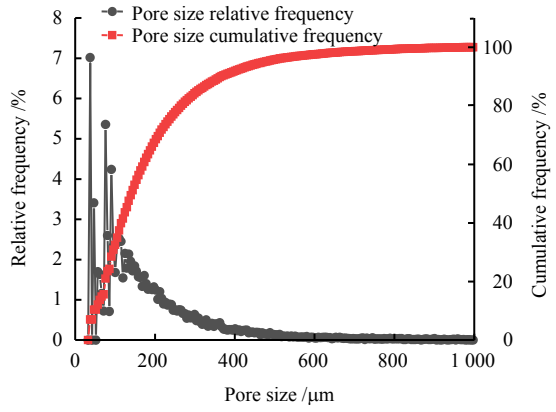

(a) Pore size distribution at 0% addition

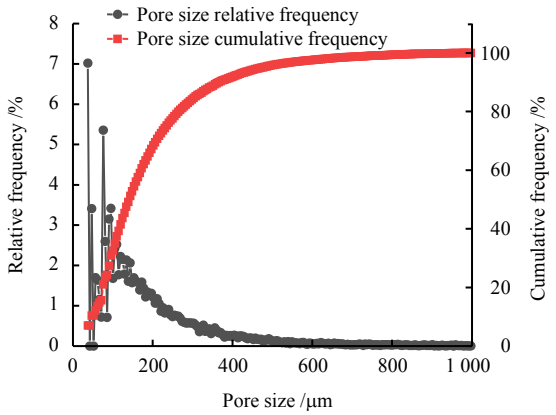

(b) Pore size distribution at 5% addition

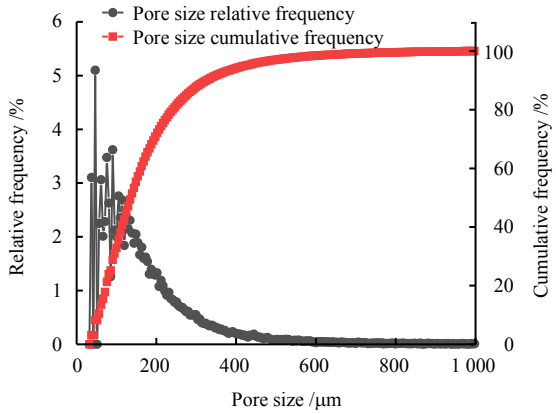

(c) Pore size distribution at 10% addition

Fig. 7 Backfill pore size distribution with different additive amounts

Figure 7 shows that the pore size distribution characteristics of the backfill when the additive amount of BS/EP-CPCM is 5% are almost the same as those without addition, and the main pore size distribution range is 35–150 μm; when the additive amount increases to 10%, the relative proportion of pore size distribution reduces, and the main pore size distribution range becomes 35–200 μm. The main reason is that with the increase of BS/EP-CPCM, there are large pores in the added porous medium, and the distribution of each pore size is relatively more uniform.

(3) Three-dimensional shape of macropores

Although the shape of the pores can be roughly regarded as a sphere, the pore shape is actually not a regular sphere but more complicated. In order to characterize the three-dimensional shape of the pore, sphericity can be used to describe the true shape of the pore. The calculation formula for sphericity S is

$$S = \frac{\pi^{\frac{1}{3}}(6\times V)^{\frac{2}{3}}}{A} \tag{1}$$

where V is the three-dimensional volume of the pore; A is the three-dimensional surface area of the pore. Both V and A can be obtained from the CT scanning results. Figure 8 shows the comparison of the sphericity of the phase change backfill with three different additive amounts of BS/EP-CPCM.

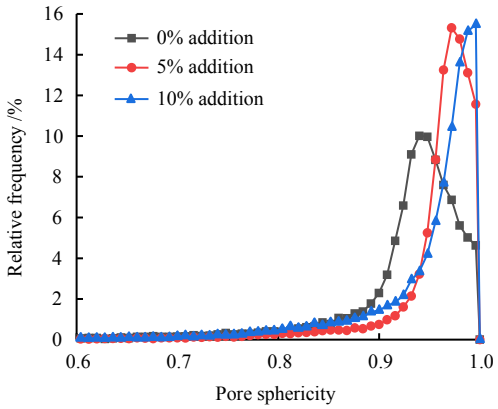

Fig. 8 Backfill pore sphericity with different additive amounts

The closer the pore sphericity is to 1, the closer the pore shape is to a sphere. As shown in Fig. 8, when the additive amount is 0%, the sphericity of pores of the backfill concentrates around 0.95; when the additive amount is 5%, the sphericity is mainly distributed around 0.97; when the additive amount is 10%, the sphericity concentration value almost reaches 0.99, which means that most of the pores are in the shape of a sphere. With the increase of the BS/EP-CPCM addition, the pore sphericity concentration range of the backfill gradually approaches 1, namely, the pore shape is closer to a sphere, and the proportion of pores with sphericity close to 1 gradually increases. The inferred reason is

that the pores in the porous medium are mostly regular, while there are more irregular pores in the backfill. With the increase of BS/EP-CPCM, the number of pores increases greatly, and the proportion of regular pores in the porous medium also increases, and the sphericity of the pores tends to be 1.

3.1.3 Macropore connectivity characteristics

In addition to the basic characteristics of pores, CT scanning can also achieve pore connectivity properties, which are characterized by the parameters of pore throats, mainly including the number of pore throats, length, radius, and coordination number. The relevant pore throat parameters of the three different BS/EP-CPCM phase change backfills are shown in Table 2.

Compared with the original backfill, the number, average length and radius of pore throats after adding BS/EP-CPCM are greatly increased, and the pore connectivity is greatly improved. When the additive amount is 10%, although the number of pore throats is less compared with the additive amount of 5%, both the average radius and length of the pore throats increase, and the connectivity is also greatly improved. Next, the frequency distributions of throat radius, length and coordination number will be analyzed respectively.

Table 2 Backfill pore throat parameters with different additive amounts

BS/EP-CPCM additive amount /%	Number of pore throats	Average throat length /μm	Average throat radius /μm	Ratio of throat length to radius
0	6 389	481.9	44.4	10.9
5	58 009	1 252.7	76.7	16.3
10	40 700	1 607.9	168.3	9.6

(1) Throat radius

The pore throat radius distributions of different BS/EP-CPCM additive amounts are shown in Fig. 9.

From Fig. 9, when the additive amount of BS/EP-CPCM is 0%, the throat radii are mainly distributed in the range of 0 to 50 μm; when the additive amount is 5%, the throat radii mainly fall in the range of 0 to 100 μm; and when the additive amount is 10%, the range becomes 0 to 200 μm and the relative frequency peak value drops from 29% to 10%. It can be seen that with the increase of the BS/EP-CPCM addition, the radius of the throat gradually increases, and the range of the concentration area of throat radius distribution grows, and the pore connectivity also increases. The reason is that the pore connectivity of the added porous medium is relatively high, and the pore throats are with large radii, which lead to enhanced pore connectivity.

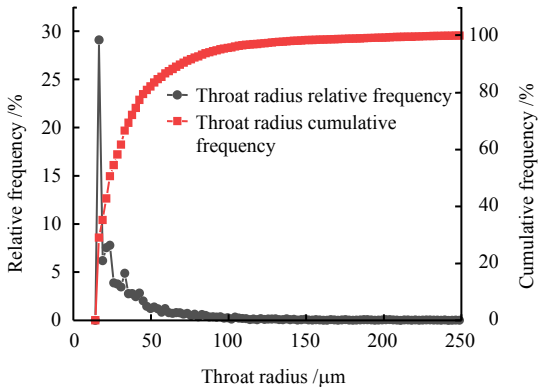

(a) Throat radius distribution at 0% addition

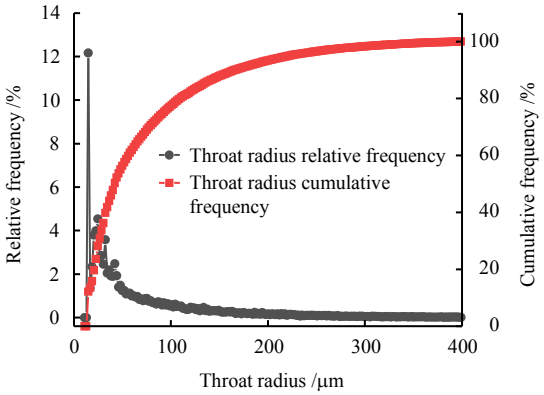

(b) Throat radius distribution at 5% addition

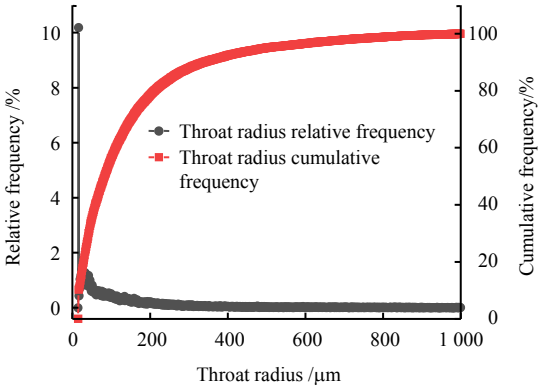

(c) Throat radius distribution at 10% addition

Fig. 9 Distribution of pore throat radius of backfill with different additive amounts

(2) Throat length

Figure 10 shows the pore throat length distributions of the phase change backfill with different BS/EP-CPCM additive amounts.

It can be seen from Fig. 10 that the throat length of the backfill is obviously increased after adding BS/EP-CPCM compared with the original backfill without additive. However, the pore throat length distribution of the backfill when the additive amount of BS/EP-CPCM is 10% is similar to that when the additive amount is 5%, with a majority of the throats having lengths less than 2 mm, in addition to a small percentage having relatively big lengths. The reason is that the added porous medium has similar internal pore connectivity,

namely, except for some long pore throats, most of the others are short pore throats.

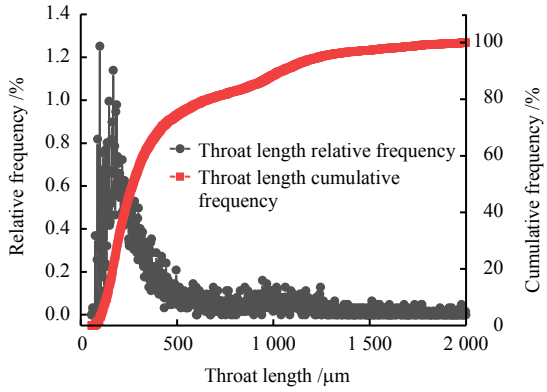

(a) Throat length distribution at 0% addition

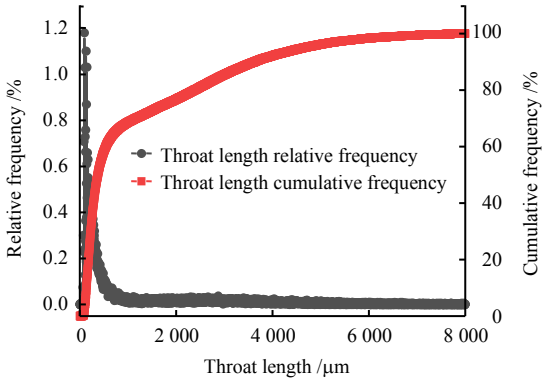

(b) Throat length distribution at 5% addition

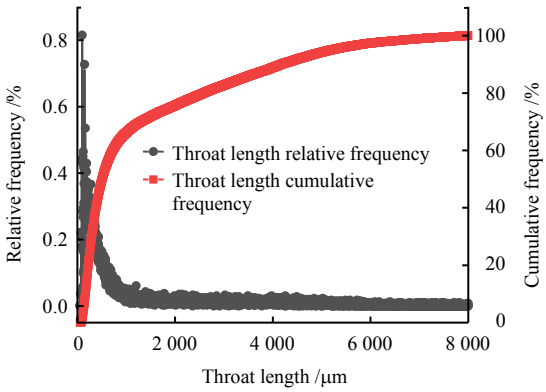

(c) Throat length distribution at 10% addition

Fig. 10 Pore throat length distribution of backfill with different additive amounts

(3) Coordination number

The coordination number is a parameter describing the number of pore throats connected to each pore. The comparison of the pore coordination number of the backfill with different additive amounts is shown in Fig. 11.

From Fig. 11, it can be seen that the pore coordination number distributions of phase change backfill with different BS/EP-CPCM additions are similar, most of the coordination number values are concentrated below 5, and a small part of coordination number are in the range of 5 to 30. The reason for the difference in connectivity of phase change backfill is that the coordination numbers of the pore throats in the added porous medium are almost the same, and those numbers are relatively low in the slurry, leading to a similar coordination number distribution in the phase change backfill.

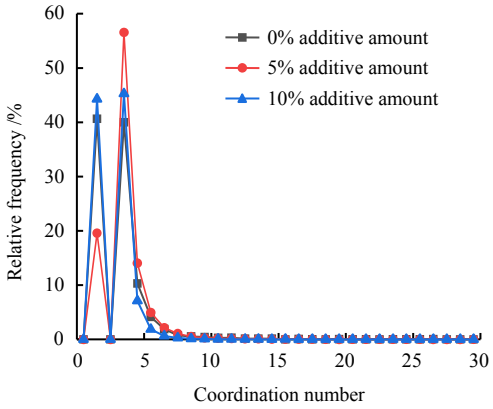

Fig. 11 Pore coordination number of backfill with different additive amounts

3.1.4 Macropore fractal dimension

In addition to the basic characteristics and connectivity characteristics of pores, fractal dimension is also an important indicator of pore characteristics, which can effectively reflect the fractal characteristic of rock pore structure. The CT scanning image is first binarized using Matlab, and the box-counting dimension method is used to perform the calculation. Since the two-dimensional fractal dimension describes the distribution characteristics of a certain section, one per every 100 slices is selected for characterization from a total of 3 744 slices in the *z*-direction of the cylindrical specimen, and the average value of the fractal dimension numbers for the middle 34 slices is taken. Figure 12 shows the comparison of the fractal dimension numbers of the phase change backfill obtained with different BS/EP-CPCM additions.

It can be seen from Fig. 12 that the fractal dimension of the backfill decreases by about 0.7 after adding 5% BS/EP-CPCM, which means the pore structure of the original backfill is more complicated than the phase change backfill when the additive amount is 5%. The reason is that the pore size of the original backfill is relatively small, and the distribution is more complicated. When the additive amount increases to 10%, the fractal dimension increases to 1.77. The reason is that, with the increase of BS/EP-CPCM, the number of pores in the porous medium increases significantly, resulting in an increasing complexity of pore structure distribution within the phase change backfill.

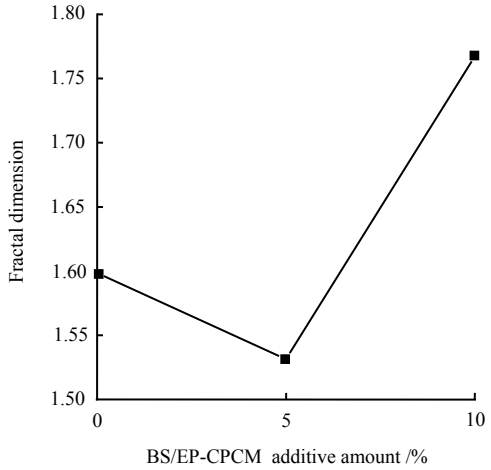

Fig. 12 Fractal dimension of backfill with different additive amounts

3.2 Pore characteristics obtained by MRI

The MRI can detect the signal intensity of water in each pore and the signal intensity of water in all pores. The ratio between them can characterize the proportion of the pores with different sizes to the total pores in the rock, namely, the pore size distribution. Due to the limitation of the CT scanning resolution, it is impossible to obtain the characteristics of the pores with the pore size smaller than 31.4 μm. MRI can completely obtain pore characteristics including micropores, mesopores, and macropores, and thus, MRI is used to obtain the porosity and pore size distribution characteristics of the phase change backfill to complement the results obtained by CT scanning.

3.2.1 Porosity obtained by MRI

Table 3 shows the average porosities of the phase change backfills with three different additive amounts obtained by MRI.

Table 3 Porosity of phase change energy storage backfill with different additive amounts

BS/EP-CPCM additive amount /%	Porosity /%
0	3.30
5	6.67
10	12.36

It can be seen from Table 3 that with the increase in the additive amount of BS/EP-CPCM, the porosity of the backfill gradually increases. Since the pores with the size below 31.4 μm are also widely distributed in the backfill, the porosities covering the statistics of micropores and mesopores are larger than those obtained by CT scanning. When the additive amounts of BS/EP-CPCM are 0%, 5% and 10%, the porosities obtained by MRI increase by 2.77%, 2.06% and 3.44% respectively compared with the porosities obtained by CT scanning. The reason is that the micropores in the filling slurry are partially compressed after adding the BS/EP-CPCM, but with the increase of the additive amount, the content of expanded perlite with micropores increases, which results in the increase of the proportion of the overall micropores.

3.2.2 Pore size distribution obtained by MRI

Figure 13 shows the pore size distributions of the phase change backfills with three different additive amounts obtained by MRI.

It can be seen from Fig. 13 that with the increase of BS/EP-CPCM addition, the pore size distribution of the phase change backfill gradually shifts to large pore size, and the proportion of large-diameter pores in the backfill gradually increases. In addition, the distribution frequency in the pore-size range of 10–100 μm increases with the increase of the additive amount, which is consistent with the law obtained by CT scanning that the distribution frequency in the pore-size range of 31.4–200 μm increases with the increase of the additive amount.

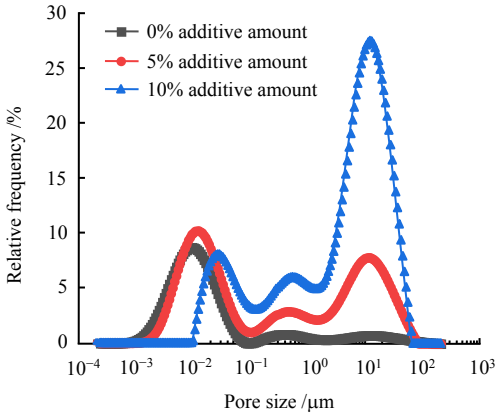

Fig. 13 Backfill pore size distribution with different additive amounts

3.3 Analysis of compressive strength and deterioration mechanism of backfill

3.3.1 Uniaxial compressive strength

The unconfined compression test was performed on the backfill specimens with different additive amounts using a compression testing machine, and the comparison of the uniaxial compressive strengths of the specimens is shown in Fig. 14.

It can be seen from Fig. 14 that the strength of the phase change backfill gradually decreases with the increase of the additive. When the additive amount of BS/EP-CPCM is 0%, the uniaxial compressive strength of the backfill is 3.64 MPa; when the additive amount is 5%, the uniaxial compressive strength of the backfill is 2.54 MPa, which drops by 30.2% compared with the strength of the backfill of 0% addition; when the additive amount is 10%, the uniaxial compressive strength of the backfill is 1.86 MPa, which is 48.9% lower than the strength when the additive amount is

0%, and 18.7% lower compared with the backfill of 5% addition. This means that the backfill strength is greatly reduced by adding the BS/EP-CPCM, but the strength deterioration rate decreases as the addition amount increases.

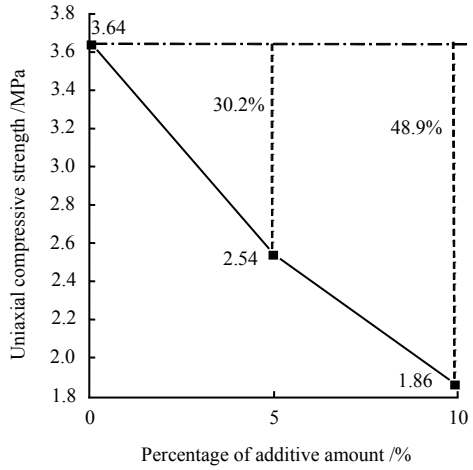

Fig. 14 Uniaxial compressive strength of backfill with different additive amounts

3.3.2 Backfill strength deterioration mechanism analysis

Combining with the pore characteristics of the phase change backfills with different BS/EP-CPCM additions obtained by CT scanning and MRI, as well as the changing law of the backfill strength, the deterioration law of the backfill strength is investigated.

With the addition of BS/EP-CPCM increasing from 0% to 10%, the backfill porosity gradually increases, and the increase amplitude is small at first and then becomes large. Since the micropores (<1 μm) have little effect on the strength of the backfill, the influence of mesopores (1–10 μm) and macropores (>10 μm) are mainly considered. The mesopore ratio and macropore ratio increase approximately linearly with the increase of additive amount, their distribution frequency will increase accordingly, and the pore shape is gradually close to a sphere. The number of pores will increase greatly when the amount of BS/EP-CPCM is 5%, and increase slightly when the additive amount is 10%, and the connectivity of the pores will gradually increase with the increase of the additive amount. As the additive amount increases, under the influence of the pores in the added porous medium, the pore distribution of the phase change backfill will be relatively concentrated at first and then complicated.

The reason is that compared with the phase change backfill without addition, there are more micropores at the bonding area between the expanded perlite particles and the filling slurry in the phase change backfill with 5% BS/EP-CPCM addition, and there are still some micropores in the expanded perlite though a part of internal pores are filled with the phase change material. As the addition of BS/EP-CPCM continues to increase, the number and volume of micropores at the bonding area between expanded perlite particles and filling slurry decrease, and the internal pores of expanded perlite become the main component composing the pores of the phase change backfill.

Comparing the deterioration trend of the backfill strength with the pore characteristics of the phase change backfill with different BS/EP-CPCM additive amounts shows that when the addition of BS/EP-CPCM is 5%, the backfill will be affected by the increase of the number of macropores, and the strength will be greatly reduced. The water conductivity and crack propagation also lead to rapid strength deterioration due to the increase in pore connectivity. However, as the addition amount of BS/EP-CPCM continues to increase, the pore size distribution of the backfill tends to be uniform, and the number of pores increases slightly. Although there are large-diameter pores in the added BS/EP-CPCM, the effect of the large-diameter pores is relatively small since a large number of ordinary pores mitigate the impact; in addition, the connectivity of the pores will be further increased, the pore distribution will be more complex, and the impact on the strength of the specimen will be small. Therefore, the increased deterioration effect of 10% additive amount is reduced compared with that of 5% additive amount. If the additive amount of BS/EP-CPCM continues to increase, the strength of the backfill will be further reduced by the increased porosity, but the reduce rate decreases.

4 Conclusion

Through CT scanning, MRI imaging and uniaxial compressive strength testing of the phase change backfills with different BS/EP-CPCM additive amounts, the pore characteristics of the phase change backfills and the conclusions of their influence on strength are as follows:

(1) With the addition amount of BS/EP-CPCM increasing from 0% to 10%, the porosity of the phase change backfill gradually increases from 3.3% to 12.36%, the macropore rate increases approximately linearly, and the pore shape tends to be sphere.

(2) With the increase of the additive amount of BS/EP-CPCM, the pore connectivity of the backfill gradually increases, the pore throat length increases, and the number of macropores increases. The pore throat coordination number is concentrated below 5, the fractal dimension drops first and then rises sharply,

and the pore distribution is more complex.

(3) Compared with the backfill without addition, the strength of the backfill with 5% addition decreases by 30.2% due to the increase of macropores and pore connectivity; when the addition amount is 10%, the pore size distribution tends to be uniform, and the strength decreases by 48.9%.

(4) Comprehensively combining the strength and pore characteristics of the phase change backfills with different BS/EP-CPCM additive amounts, it can be concluded that if the BS/EP-CPCM is applied to backfill projects of mines, the appropriate additive amount is about 5%. Future studies will further investigate the pore characteristics to obtain the methods that can reduce the strength degradation effect of the additive amount of phase change material on the backfill.

References

[1] LIU Lang, XIN Jie, ZHANG Bo, et al. Fundamental theory and application exploration of mine functional filling[J]. Journal of China Coal Society, 2018, 43(7): 1811−1820.

[2] ZHANG Xiao-yan, XU Mu-yan, LIU Lang, et al. Experimental study on thermal and mechanical properties of cemented paste backfill with phase change material[J]. Journal of Materials Research and Technology, 2020, 9(2): 2164−2175.

[3] CUI Hong-zhi, SHAZIM ALI MEMON, LIU Ran. Development, mechanical properties and numerical simulation of macro encapsulated thermal energy storage concrete[J]. Energy and Buildings, 2015, 96: 162−174.

[4] KASTIUKAS G, ZHOU X, CASTRO-GOMES J. Development and optimisation of phase change material-impregnated lightweight aggregates for geopolymer composites made from aluminosilicate rich mud and milled glass powder[J]. Construction and Building Materials, 2016, 10: 201−210.

[5] MA Qin-yong, BAI Mei. Mechanical behavior, energy-storing properties and thermal reliability of phase-changing energy-storing concrete[J]. Construction and Building Materials, 2018, 176: 43−49.

[6] SANG Guo-chen, FAN Min, CUI Xiao-ling, et al. Thermal and mechanical properties of pressure molded phase change energy storage mortar[J]. Journal of Building Materials, 2019, 22(5): 693−699.

[7] GU Wan-qing. Preparation and experimental analysis of lauryl alcohol/expanded perlite phase change energy storage concrete[D]. Huainan: Anhui University of Science and Technology, 2019.

[8] WANG Zhen-shuang, HU Min. Preparation and properties of composite phase change energy storage mortar[J]. Journal of Basic Science and Engineering, 2016, 24(2): 315−321.

[9] JIANG Ming-jing, WU Di, CAO Pei, et al. Analysis of connected pores of calcareous sand based on SEM images[J]. Chinese Journal of Geotechnical Engineering, 2017, 39(Suppl.1): 1−5.

[10] ZHAO Yi-qing, WU Chang-gui, JIN Ai-bing, et al. Experimental study on microstructure and mechanical properties of heat-treated sandstone[J]. Rock and Soil Mechanics, 2020, 41(7): 2233−2240.

[11] LIU Bo, SUN Yan-ding, YUAN Yi-feng, et al. Strength characteristics and strengthening mechanism of frozen sandstone with different water contents[J]. Journal of China University of Mining and Technology, 2020, 49(6): 1085−1093, 1127.

[12] JIN Ai-bing, WANG Shu-liang, WEI Yu-dong, et al. Influence of different cooling conditions on physical and mechanical properties of high-temperature sandstone[J]. Rock and Soil Mechanics, 2020, 41(11): 3531−3539, 3603.

[13] YANG Hong-rui, LIU Ping, SUN Bo, et al. Study on the damage mechanism of microstructures of conglomerate sandstone in Maijishan Grottoes by freeze-thaw cycles[J]. Chinese Journal of Rock Mechanics and Engineering, 2021, 40(3): 545−555.

[14] WANG Ben-xin, JIN Ai-bing, ZHAO Yi-qing, et al. Experimental study on fracture rule of 3D printed specimens with non-hole-through joints based on CT scan[J]. Rock and Soil Mechanics, 2019, 40(10): 3920−3927, 3936.

[15] WU Fa-quan, QIAO Lei, GUAN Sheng-gong, et al. Uniaxial compression test study on size effect of small size rock samples[J]. Chinese Journal of Rock Mechanics and Engineering, 2021, 40(5): 865−873.

[16] SIRDESAI N N, SINGH T N, GAMAGE R P. Thermal alterations in the poro-mechanical characteristic of an Indian sandstone−a comparative study[J]. Engineering Geology, 2017, 226: 208−220.

[17] FU Yu, FENG Zhong-liang, LI Pei-chan. CT scanning based coal and rock heterogeneity characteristics and numerical analysis of reconstruction model[J]. Journal of Mining and Safety Engineering, 2020, 37(4): 828−835.

[18] LIU Bo, MA Ren-ming, FAN Hao-ming. Evaluation of the impact of freeze-thaw cycles on pore structure characteristics of black soil using X-ray computed tomography[J]. Soil and Tillage Research, 2021, 206: 1−11.

[19] CUI Xiang, HU Ming-jian, ZHU Chang-qi, et al. Study

on microscopic characteristics of three-dimensional pores of coral sand[J]. Rock and Soil Mechanics, 2020, 41(11): 3632−3640, 3686.

[20] XIE Chao-yang, ZHANG Wei, YAO Dong-fang, et al. Quantitative characterization of soil spatial pore network based on maximum-sphere algorithm[J]. Journal of Engineering Geology, 2020, 28(1): 60−68.

[21] CHEN Jie-jing, QIN Yong-jun, XIAO Jian-zhuang, et al. Study on pore characteristics of recycled concrete mixed with lithium slag based on CT technology[J/OL]. Journal of Building Materials, 2020:1-15[2021-03-21]. http://kns.cnki.net/kcms/detail/31.1764.tu.20201030.1522.002.html.

[22] CHEN Feng-bin, XU Bin, JIAO Hua-zhe, et al. Fiber distribution and pore structure characterization of basalt fiber reinforced concrete[J]. Journal of China University of Mining and Technology, 2021, 50(2): 273−280.

[23] WANG Deng-ke, ZENG Fan-chao, WANG Jian-guo, et al. Study on dynamic evolution characteristics and fractal law of crack in coal sample under load by microindustrial CT[J]. Chinese Journal of Rock Mechanics and Engineering, 2020, 39(6): 1165−1174.

[24] PENG Rui-dong, YANG Yan-cong, JU Yang, et al. Fractal dimension calculation of rock pore based on gray CT image[J]. Chinese Science Bulletin, 2011, 56(26): 2256−2266.

[25] GERKE K M, SIZONENKO T O, KARSANINA M V, et al. Improving watershed-based pore-network extraction method using maximum inscribed ball pore-body positioning[J]. Advances in Water Resources, 2020, 140: 103576.

[26] WILDENSCHILD D, SHEPPARD A P. X-ray imaging and analysis techniques for quantifying pore-scale structure and processes in subsurface porous medium systems[J]. Advances in Water Resources, 2013, 51: 217−246.

[27] MULJADI B P, BLUNT M J, RAEINI A Q, et al. The impact of porous media heterogeneity on non-Darcy flow behaviour from pore-scale simulation[J]. Advances in Water Resources, 2016, 95: 329−340.

[28] KHAN Z A, ELKAMEL A, GOSTICK J T. Efficient extraction of pore networks from massive tomograms via geometric domain decomposition[J]. Advances in Water Resources, 2020, 145: 103734.

[29] JIN Ai-bing, JU You, SUN Hao, et al. Phase change energy storage strength of filling body and the thermal performance study [J/OL]. Journal of Harbin Institute of Technology, 2021:1-11[2021-04-11]. http://kns.cnki.net/kcms/detail/23.1235.T.20210331.0946.002.html.

[30] LÜ Chao, SUN Qiang. Electrical resistivity evolution and brittle failure of sandstone after exposure to different temperatures[J]. Rock Mechanics and Rock Engineering, 2018, 51(2): 639−645.